# THE GAMMA DECAY FROM THE GDR IN HIGHLY ROTATING NUCLEI AT LOW TEMPERATURE*

A. Bracco

Dipartimento di Fisica, Universitá degli Studi di Milano
and INFN, Sezione di Milano, Via Celoria 16, 20133 Milano, Italy

*(Received January 7, 2003)*

A review of some of the progress made in the study of nuclei at finite temperature and rotational frequency with the giant dipole resonance is here presented. The focus is the study of the low temperature region in connection with two different problems. The first is that of the shape and damping mechanisms of the GDR as deduced from radiative fusion among heavy ion symmetric reactions. The second is the effect of the GDR decay in the population of the superdeformed structures. Some perspectives for future works with radioactive beams will be also discussed.

PACS numbers: 21.10.Re, 23.20.Lv, 24.80.+y, 27.10.+q

## 1. Introduction

The study of the nucleus at the limits of excitation energy and angular momentum is one of the central topics currently addressed with selective-spectroscopy measurements. In these extreme regimes nuclear structure studies are probing nuclear shapes and their evolution, the influence of thermal environments on low lying modes and on collective rotation and giant resonances. In particular the investigation of the simplest collective modes as a function of temperature and angular momentum have improved the knowledge of the properties of highly excited nuclei. In terms of the thermal response the emphasis is how the elementary modes of excitations are modified by thermal energy. In this connection the transition from order to chaos is investigated through the analysis of the quasi-continuum spectra formed by transitions among states of excited rotational bands with energy extending up to 4–5 MeV above the yrast line. The nuclear properties at higher excitation energies are instead explored through the $\gamma$-decay of the giant dipole resonance, excitation which can be built on any nuclear state.

* Presented at the XXXVII Zakopane School of Physics “Trends in Nuclear Physics”, Zakopane, Poland, September 3–10, 2002.

So far the GDR built on excited states has been studied extensively and has provided information on how the nuclear shape evolves with temperature and angular momentum (see [1] for a review). The measurements indicate that the resonance FWHM becomes broader as a function of both angular momentum and excitation energy. The centrifugal force induced by high rotational frequency deforms the excited nucleus and, as GDR couples to the quadrupole nuclear deformation, splits apart the GDR components therefore increasing its FWHM. Temperature, instead, controls thermal shape fluctuations that give rise to a dipole frequency distribution and, consequently, a broadening of the GDR width. The comparison between experimental data and theoretical calculations have shown that Collisional Damping, the mechanism that is responsible to the GDR width at zero temperature, is rather independent of spin and temperature (at least up to $T < 2$ MeV [2–4]).

There is an almost an unexplored region at low temperature which is interesting for the GDR properties. In fact, almost all the available data obtained so far have probed temperature regions higher than 1.2 MeV where shell effects have already vanished and the thermal fluctuations are important. Below 1.2 MeV shells and pairing play an important role and might strongly affect GDR damping mechanisms. Recently an effort has been made to populate selectively nuclei at rather low excitation energy and high finite spin by using the cold fusion in symmetric heavy ion reactions leading to compound nuclei with excitation energies of about 10 to 40 MeV. Some results concerning the $^{197}$Au nucleus are reported and discussed in Section 2.

The problem of the population of the superdeformed configurations is also studied by investigating the cooling of the residual nucleus by statistical E1. In fact, it has been predicted that one of the components of the giant dipole resonance built on very elongated shapes will be shifted to low energy, therefore strongly affecting the E1 transition probability and consequently the population of the SD states [5]. With the present data the intensity of the superdeformed yrast and excited bands is investigated when measured in coincidence with an high-energy $\gamma$-ray, to determine the importance of the E1 cooling in the feeding mechanism of the superdeformed states.

## 2. High energy photons from very symmetric reactions

A powerful way to populate selectively nuclei at rather low excitation energy and finite spin is to use the cold fusion in symmetric heavy ion reactions which lead to compound nuclei with excitation energies of about 10 to 40 MeV. Besides, in the case of symmetric reactions induced by $^{90}$Zr beams one can also exploit the fact that associated with the complete-fusion products there is the exclusive emission of $\gamma$-rays, *i.e.* radiative capture, which has been found to occur with unexpectedly large cross section (several tenths of microbarn) [6]. The first spectroscopic investigations of the radiative fusion reaction $^{90}$Zr+$^{90}$Zr was based on measured $\gamma$-rays spectra which extend up to $E = 6$–7 MeV [7]. That experiment gave only some indications on the nature of the emission of high-energy $\gamma$-rays, which seemed to result from an equilibrated compound nucleus but it was not possible to deduce information about the GDR line-shape. More recently an experiment has been made at the Argonne National Laboratory measuring high-energy $\gamma$-rays up to 14 MeV emitted in the radiative fusion reaction $^{90}$Zr+ $^{89}$Y at $E_{\rm beam} = 352$ MeV. Such measurement provides the first investigation in the temperature region $T = 0.5$–1 MeV at finite spin $I = 15$–20 $\hbar$. In that experiment the recoiling products passed through the Mass Analyzer (FMA) while the $\gamma$-rays emitted by the reaction were measured with a set up of $BaF_2$ detectors from the ORNL/MSU/TAMU array grouped in 4 packs each consisting in 37 crystals. In addition, low-energy $\gamma$-rays were also detected by a BGO spin/sum-energy array (with honeycomb structure ) which was used primarily as a multiplicity filter. The low energy $\gamma$-ray fold spectra measured in the BGO multiplicity filter in coincidence with the different recoils were found to show a behavior consistent with the statistical nature of the radiative fusion.

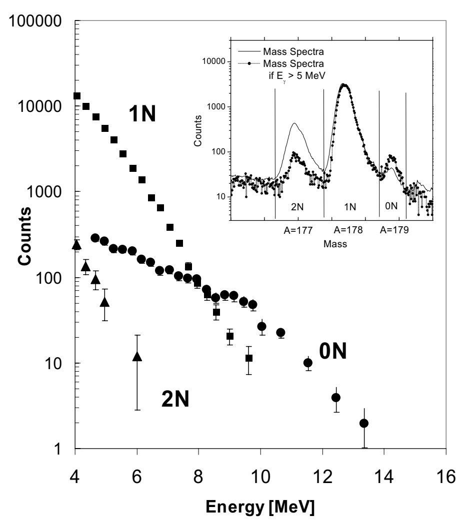


Fig. 1. The high-energy $\gamma$-rays spectra associated with the 0-, 1- and 2-nucleon emission channels (filled points, squares and triangles, respectively). In the inset the mass distributions of the residue nuclei with (circles) and without (continuous line) the requirement of a coincidence with high-energy $\gamma$-rays are shown. The spectra have been normalized to the counts of the $A = 178$ peak.

The high-energy $\gamma$-rays spectra measured in the $BaF_2$ detectors of the LEPPEX array associated to the three different recoil masses measured in the FMA are displayed in figure 1. In the inset the mass spectra are also shown. The spectrum corresponding to the 2 nucleon emission channel is very steep and dies out at rather low energy in contrast to those corresponding to the 1 and 0 particle emission channels which extend at higher energy and are characterized by very different spectral shapes. In particular, the 0-particle emission spectrum is much less steep and therefore has an enhanced sensitivity to the details of the low energy tail of the line shape of GDR built on the compound nucleus. The measured high-energy $\gamma$-ray spectra of figure 1 have been analyzed within the framework of the Monte Carlo statistical model decay of the compound $^{179}$Au nucleus. The calculations were performed assuming a level density parameter $a = A/8$ MeV$^{-1}$ and 100% of the EWSR strength of the GDR. In addition for the Yrast line the parabolic parametrization deduced from the Yrast line of Ref. [8] was used. The GDR centroids and widths were deduced using the Hill–Wheeler

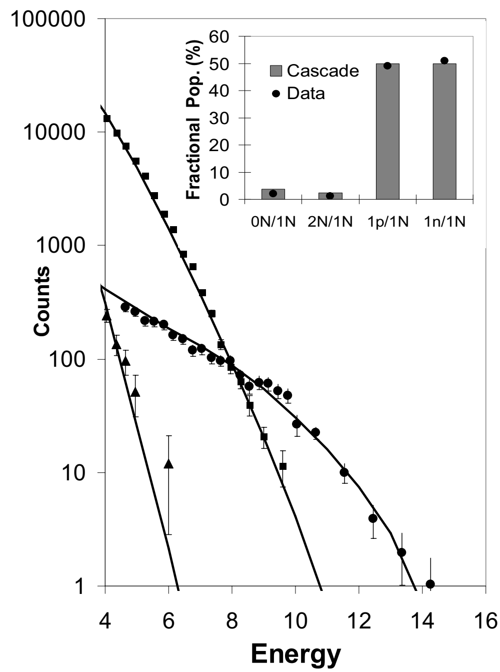


Fig. 2. The high-energy $\gamma$-ray spectra associated with the 0-, 1- and 2-nucleon emission channels (filled points, squares and triangles, respectively) are shown in comparison with statistical model calculations as described in the text. In the inset the measured fractional populations of the different residual nuclei are shown in comparison with the best fitting statistical model predictions.

parametrization of Refs [9] and [10] with the spherical value $E_0 = 14.2$. The used relation between the total width $\Gamma$ and the intrinsic width $\Gamma_0$ is $\Gamma = \Gamma_0\ (E_{\rm GDR}/E_0)^{1.6}$ [2].

In figure 2 the best fitting calculations corresponding to the quadrupole deformation parameter $\beta = 0.1$ and GDR intrinsic width of 5 MeV are shown in comparison with the data. In the inset on the figure the measured and calculated cross sections for the different residual nuclei are shown. The good agreement gives confidence that the choice of the parameters entering in the statistical model and not related to the GDR is rather good. The effective deformation deduced from the GDR is very similar to that deduced from the measurement of the yrast line transitions of the $^{179}$Au nucleus [8] and this agreement indicates the survival of shell effects in the temperature interval $T = 0.5$–1 MeV. Because of the small size of the deformation it is not possible with the present data to distinguish between an oblate or prolate deformation.

## 3. Effect of E1 decay in the population of super deformed structures

A relevant open question concerning the problem of superdeformation is the understanding of the conditions which favor the population of SD states at the highest spins, as compared to the discrete line intensities observed in normally deformed nuclei at the same highest spin values [5,11]. It has been suggested that such intense population of the SD band at high spins can be related to the E1 feeding of these states, which is expected to be strongly affected by the shape of the giant dipole resonance (GDR) strength function in the low-energy tail (namely at $E_\gamma$ lower than the neutron binding energy). This explanation was originally formulated in connection with the population of the SD nucleus $^{152}$Dy [5]. To provide a very stringent experimental test of this mechanism one needs to study the populations of the SD structures as a function of coincident high-energy $\gamma$-rays. In fact, in this way it is possible to verify whether or not the population of the SD structures increases with $\gamma$-ray energies, as expected from the GDR line shape built on a superdeformed nucleus. This is in general a difficult experimental task, due to both the exponential decrease of the yield of the high-energy $\gamma$-rays and to the weak intensity of the SD transitions, being of the order of few percent for the yrast band.

In order to address this problem we have measure SD transitions (yrast and quasi-continuum) in coincidence with high energy $\gamma$-rays and we have studied the dependence of their intensity as a function of the high $\gamma$-ray energy in the interval 3–8 MeV [5]. This is the region where one can probe the low energy tail of the GDR strength function, which in the case of a SD prolate nucleus is characterized by a double Lorentzian shape with one third of the strength expected to be around 10.5 MeV.

The experiment was performed at the Tandem Accelerator Laboratory of Legnaro (Padova, Italy). The nucleus $^{143}$Eu was populated by the fusion reaction $^{37}\mathrm{Cl} + ^{110}\mathrm{Pd} \rightarrow ^{143}\mathrm{Eu} + 4n$, at beam energies of 165 MeV. Low energy $\gamma$-rays were detected in the EUROBALL array, where the thirty tapered Ge detectors in the forward hemisphere were replaced by the eight large volume $BaF_2$ scintillators of the HECTOR detector for high energy detection [13]. The $BaF_2$ detectors were placed at 30 cm from the target to allow for a good neutron rejection by time of flight measurement relative to four additional small $BaF_2$ detectors, used as a time reference. The SD yrast band intensity is shown in figure 3 for the following two gating conditions on the high energy $\gamma$-ray detected in the $BaF_2$ scintillators: panel (a) 3 MeV $< E_\gamma <$ 4 MeV with average energy $\langle E_\gamma \rangle = 3.4$ MeV and panel (b) 6 MeV $< E_\gamma <$ 14 MeV with average energy $\langle E_\gamma \rangle = 7.3$ MeV. Each spectrum is also gated on low energy SD yrast $\gamma$-rays, and Doppler corrected by taking into account the energy dependent fractional Doppler shift. The spectra have been normalized to the intensity of the 917 keV low energy transition

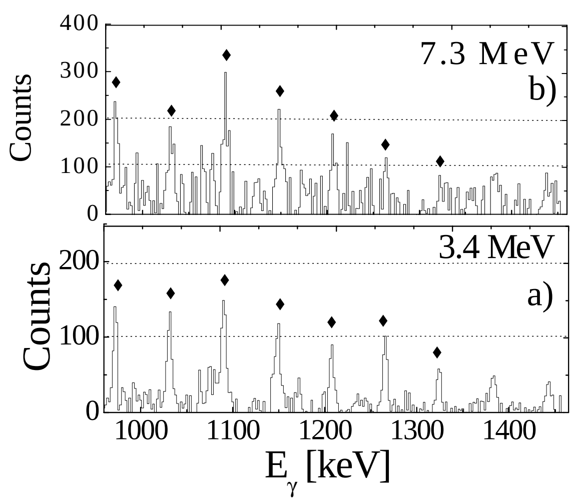


Fig. 3. Spectra of the SD yrast of $^{143}$Eu, gated by high-energy $\gamma$-rays with average energies $\langle E_\gamma \rangle = 3.4$ (panel (a)) and 7.3 MeV (panel (b)). The spectra are normalized to the intensity of the low spin 917 keV line, with the gating condition $\langle E_\gamma \rangle = 7.3$ MeV. The diamonds indicate the SD lines used to calculate the increase of the yrast intensity.

between spherical states, to allow for a comparison of the superdeformed band population. The increase of the intensity with increasing high energy gating, already visible in the figure, has been estimated by summing the intensity of the marked peaks. This has given a factor of 1.6 increase between the lowest and the highest gating condition, as discussed in connection with figure 5.

The feeding properties of the superdeformed unresolved transitions have also been studied. In $^{143}$Eu a continuous distribution of superdeformed character, corresponding to damped transitions at higher excitation energy, has also been observed in the region $1200 < E_\gamma < 1700$ keV [14]. It has been found that the intensity of such superdeformed E2 bump is much stronger for transitions leading to the population of the low spin spherical (ND) structure as compared to that leading to the low spin triaxial (TD) shape. Figure 4 shows the spectra emphasizing the region of the E2 continuum, normalized on the 553 keV low spin spherical transition. To isolate in the best possible way the expected contribution from the superdeformed component only, we have evaluated the excess yield of the ND bump as compared to the TD bump, as shown in the top panel of Fig. 4. Again, one clearly observes that the SD contribution to the continuum spectrum increases with the energy of the high energy gate.

Figure 5 shows the summary of the results concerning the SD structures by presenting in addition to the SD yrast data those concerning the SD ridges and E2 bump. Altogether, it is clear that the measured increased for the ridges and E2 bump is consistent with that of the SD yrast, therefore supporting the SD nature of these structures. To model in a rather realistic way the complex $\gamma$-decay flow from the entry distribution of the residual nucleus down to the yrast line, we have also performed schematic Monte Carlo calculations. The adopted model has earlier been used to describe the populations of the various spectral component of the SD nucleus $^{143}$Eu, giving a good account for the experimental data [15,16]. The model is based on the level densities of both ND and SD states, together with the E1 and E2 transition probabilities characteristic of the two deformed shapes. In the case of ND states the level density is described by the Fermi-gas expression, with a level density parameter $a_{\rm ND} = A/10$, while the level density of SD states is taken from the cranking + band mixing calculations of Ref. [17] (corresponding roughly to a level density parameter $a_{\rm SD} = A/18.6$). In the code, the two deformations are separated by a barrier, the tunneling through which allows the mixing between SD and ND states. In particular, the statistical E1 strength entering into the simulation is described as the tail of the giant dipole resonance of Lorentzian shape, with centroids and widths for the SD and ND configurations, as given above.

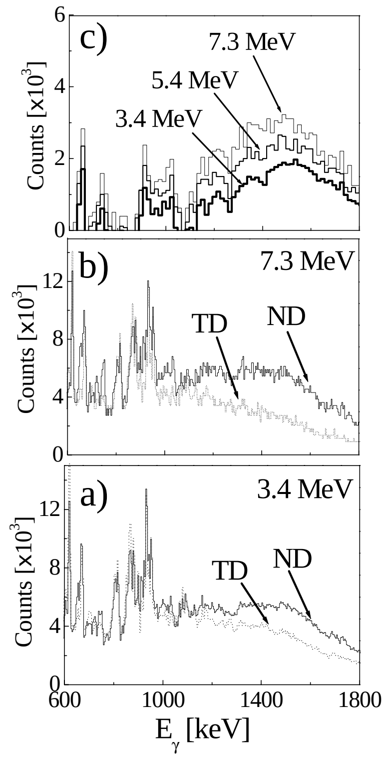


Fig. 4. Spectra of $^{143}$Eu collecting the entire decay flow (ND) and the triaxial contribution only (TD), gated by high-energy transition with $\langle E_\gamma \rangle = 3.4$ (panel (a)) and 7.3 MeV (panel (b)). The intensity of the E2 bump observed in the ND spectra, obtained as a difference between the ND and TD spectra and normalized to the intensity of the 553 keV low spin spherical transition, is shown in the top part of the figure.

The parameters used in the calculations are the same as discussed in Ref. [16], with the only difference for the entry excitation energy, which was 4 MeV in the previous case and it has now been increased by 5 MeV to match the new experimental condition. This corresponds to an average entry energy of 9 MeV above yrast.

In order to rule out possible spin effects, for which we know that an increase of spin induces an increase of the population, we have measured the average multiplicity, which reflects the average spin, as a function of the high-energy gating $\gamma$-ray transition (top panel of figure 5). In the present case, an opposite situation is found, since the increase of the SD population is observed to be associated with a decrease of the average spin of approximately 8 units, as deduced from the multiplicity measurement. It is also

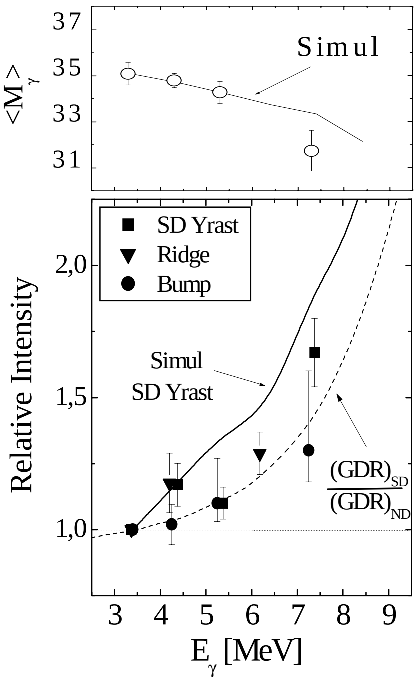


Fig. 5. The bottom part of the figure shows the intensity of the SD yrast (squares), of the SD ridge (filled triangles) and of the E2 bump (filled circles), as function of the energy of the gating transition, relative to the corresponding values measured at $\langle E_\gamma \rangle = 3.4$ MeV. The dashed line corresponds to the ratio of the strength functions of the GDR built on a SD and a ND nucleus, while the full line gives the predicted values of the relative intensity of the SD yrast, as obtained from the model described in the text. In the top part of the figure the total average multiplicity of the $\gamma$-cascades leading to $^{143}$Eu is shown for both the experimental data (circles) and the model, as function of the energy of the gating transition.

found that the value of the multiplicity deduced from the schematic Monte Carlo calculations reproduces rather well this observed decrease. Altogether one can say that we have found an increase of SD transitions intensity and a decrease of the average $\gamma$-multiplicity with increasing high energy $\gamma$-ray gates, which are both well reproduced by the same simulation calculations.

One can then conclude that the feeding intensity of the superdeformed states, including the damped transitions from the E2 continuum, is almost a factor of 1.6 larger when gating on high energy $\gamma$-rays (with $E_\gamma > 6$ MeV) as compared to the ungated case. This not only clearly suggests that for $^{143}$Eu the E1 decay is the favorable mechanism for the population of SD configurations, but also supports the superdeformed nature of the rotational quasi-continuum observed in this nucleus [14]. However, in order to see whether or not this is a general feature of the feeding of the SD structures one needs more experimental work also in other region of mass where superdeformed shapes have been found.

## 4. Conclusions and some future perspectives with radioactive beams

In this talk it has been shown that the study of highly excited collective states at temperature $< 1$ MeV, has provided the opportunity to investigate few intriguing aspects of nuclear structure in extreme conditions: the role of shapes and persistence of shell effects as probed by the giant dipole resonance and the effect that the gamma decay of the GDR has in the population of superdeformed states. At higher excitation energy, particularly at temperature around 3 MeV there are other open problems in connection with the GDR line shape which are related to the fact that in this case it is more difficult to define the excitation energy of the nucleus. In fact sizable pre-equilibrium effects should be in that case accounted for. An experimental program aiming at studying this high temperature region has recently started at LNL using the GARFIELD array (see the contribution of Fabiana Gramegna to this conference).

A new program is now also being started concerning the study of the gamma-decay of E1 states in neutron rich nuclei. The giant dipole resonance in the unstable neutron rich nuclei is of particular interest because it carries useful information on the underlying nuclear structure as well as on the effective nucleon-nucleon interaction in the medium. Although this topic has attracted much attention over several past decades, in the case of nuclei far from the stability line the investigation of collective modes is still in its infancy. Recently the investigation of the giant dipole resonance in the $^{68}$Ni nucleus has been planned by using the RISING set up at GSI. To excite the giant dipole resonance use will be made of the Coulomb excitation in inverse kinematics of the beam of $^{68}$Ni at 400 MeV/u on a $^{208}$Pb target. For the $^{68}$Ni nucleus calculations (in non-relativistic and relativistic random phase approximation) predict a "pygmy" component, namely a low-lying dipole strength (at energy below 10 MeV) which is much stronger than that of the less neutron rich stable isotopes (see [18]). The investigation of the pygmy dipole resonance is interesting not only to study mean field modifications induced by large isospin in the ground state, but also for its implications in the astrophysical models predicting the element abundances in the r-process. For this experiment use will be made of both the RISING germanium cluster detectors at forward angles together with large volume $BaF_2$ detectors at the backward angles. This is expected to open a new line of research with radioactive beams.

The author would like to thank all the collaborators of this works. In particular, for the experiment on $^{197}$Au I acknowledge the active participation of F. Camera, F. Della Vedova, S. Leoni, B. Million, S. Mantovani, M. Pignanelli, O. Wieland, (from Milano); M.P. Carpenter, D. Hoffman, B.B. Back, F.G. Kondev, T.L. Khoo, C.J. Lister, A.M. Heinz, R.V.F. Janssens, D. Jenkins, T. Lauritsen, B. Mcclintock, S. Mitsuoka, E.F. Moore, D. Seweryniak, R.J. Van Swol, V. Nanal from ANL, R. Siemssen from KVI, M. Thoennessen, K. Eisenman, P. Heckman, J. Seitz, from MSU; R. Varner, M. Halbert,from ORNL, I. Dioszegi (from Stony Brook); A. Lopez-Martensg from CSNSM, Orsay. The Euroball experiment was made in collaboration with G. Benzoni, F. Camera, S. Leoni, B. Million, N. Blasi, M. Pignanelli, O. Wieland from Milano, A. Maj, M. Kmiecik, M. Zieblinski and J. Styczen from Cracow, A. Zucchiatti and M. Castoldi from Genova, A. Algora (from LNL), A. Axelsson and J. Nyberg from Uppsala, M. Bergström and B. Herskind from NBI.

## REFERENCES

[1] P.F. Bortignon, A. Bracco, R.A. Broglia, Harwood Academic Publishers, Amsterdam 1998, volume of Contemporary Concepts in Physics.

[2] W.E. Ormand *et al. Phys. Rev. Lett.* **77**, 607 (1996); *Nucl. Phys.* **A614**, 217 (1997); **A6148**, 20 (1997).

[3] A. Bracco *et al., Phys. Rev. Lett.* **74**, 3748 (1995).

[4] D. Kusnezov, Y. Alhassyd, K. Snover, *Phys. Rev. Lett.* **81**, 542 (1998).

[5] B. Herskind *et al., Phys. Rev. Lett.* **59**, 2416 (1987).

[6] J.G. Keller *et al., Nucl. Phys.* **A452**, 173 (1986).

[7] K.-H. Schmidt *et al., Phys. Lett.* **B168**, 39 (1986).

[8] W. Müller *et al.*, to be published.

[9] Y. Alhassid, *Nucl. Phys.* **A649**, 107c (1999) and references therein.

[10] W.E. Ormand, *Nucl. Phys.* **A649**, 145c (1999) and references therein.

[11] E. Vigezzi *et al., Phys. Lett.* **B249**, 263 (1990).

[12] G. Benzoni *et al., Phys. Lett.* **B540**, 199 (2002).

[13] A. Maj *et al., Nucl. Phys.* **A571**, 185 (1994).

[14] S. Leoni *et al., Phys. Rev. Lett.* **76**, 3281 (1996).

[15] K. Schiffer, B. Herskind, J. Gascon, *Z. Phys.* **A332**, 17 (1989).

[16] S. Leoni *et al., Phys. Lett.* **B409**, 71 (1997).

[17] K. Yoshida, M. Matsuo, Y.R. Shimizu, *Nucl. Phys.* **A696**, 85 (2001).

[18] G. Colo, *Acta Phys. Pol. B* **34**, 2175 (2003), these Proceedings and references therein.